

EOS Microwave Limb Sounder Observations of the Antarctic Polar Vortex Breakup in 2004

G. L. Manney,^{1,2} M. L. Santee,¹ N. J. Livesey,¹ L. Froidevaux,¹ W. G. Read,¹
H. C. Pumphrey,³ J. W. Waters,¹ and S. Pawson⁴

Abstract. New observations from the Microwave Limb Sounder (MLS) on NASA's Aura satellite give a detailed picture of the spring Antarctic polar vortex breakup throughout the stratosphere, with the first daily global HCl profiles providing an unprecedentedly clear view of transport in the lower stratosphere. Poleward transport at progressively lower levels, filamentation, and mixing are detailed in MLS HCl, N₂O, H₂O, and O₃ as the 2004 Antarctic vortex broke up from the top down in early October through late December. Improved MLS H₂O data show the subvortex, below the tropical tropopause, breaking up almost simultaneously with the lower stratospheric vortex in December. Vortex remnants persisted in MLS tracers for over a month after the breakup in the midstratosphere, but no more than a week in the lower stratosphere. MLS observations show diabatic descent continuing throughout November, but weak ascent after late October in the lower stratospheric vortex core. Our results extend previous observational transport studies and show consistency with mixing and vortex evolution in meteorological analyses, and with model studies.

1. Introduction

The spring stratospheric polar vortex breakup is important to understanding transport, especially in the southern hemisphere (SH) where ozone-depleted air may disperse throughout the hemisphere [e.g., *Ajtić et al.*, 2004]. Previous observational studies of transport during the SH vortex breakup were limited by data sparsity: Detailed analysis by *Lahoz et al.* [1996] and *Orsolini et al.* [2005] was limited to the middle and upper stratosphere by data quality. Neither could show the full period of the vortex breakup, the former because of Upper Atmosphere Research Satellite (UARS) yaw cycles, and the latter because of data gaps. *Orsolini et al.* [2005] also had to average several days' data to get low-resolution hemispheric maps. H₂O was the only long-lived tracer available for these studies. Other studies [*Ajtić et al.*, 2004, and references therein] relied on column O₃ or sparse ground-based or solar occultation profiles for obser-

vatational results.

The Microwave Limb Sounder (MLS) on NASA's Earth Observing System (EOS) Aura satellite, launched 15 July 2004, is an enhanced follow-on to the UARS MLS instrument [e.g., *Waters et al.*, 1999]. In addition to better spatial coverage, resolution, and precision, EOS MLS measures many species not available from UARS MLS, including N₂O and the first daily global profile measurements of HCl. We use N₂O, HCl, H₂O, and O₃ from EOS MLS, and NASA's Global Modeling and Assimilation Office Goddard Earth Observing System, Version 4.0.3 (GEOS-4) meteorological analyses [*Bloom et al.*, 2005], to detail the vortex breakup in SH spring 2004; our results cover the full stratosphere and time period of the final warming and include several tracers, significantly extending previous observational results.

MLS data shown are preliminary; refinements and extensive validation efforts are underway. Estimated accuracies are ~30 ppbv, 1 ppmv, 0.2 ppbv, and 0.5 ppmv for N₂O, H₂O, HCl, and O₃, respectively, for the vertical range and time period shown here. Reprocessing with improved algorithms is planned only for focused validation periods and spot checks because of computational limitations; comparison with reprocessed days shows that analyses of the prelim-

¹Jet Propulsion Laboratory, California Institute of Technology, Pasadena.

²Also at Department of Natural Sciences, New Mexico Highlands University.

³University of Edinburgh, UK.

⁴NASA/Goddard Space Flight Center

inary data capture very well the morphology and evolution of the vortex, thus our results are robust. Computational limitations barred processing every day of MLS observations; for timeseries plots, short data gaps are filled using a Kalman smoother, as in *Santee et al.* [2005].

2. The 2004 Antarctic Polar Vortex Breakup

N_2O , HCl and O_3 as a function of equivalent latitude (EqL, the latitude enclosing the same area as a given potential vorticity, PV, contour) and potential temperature (Figure 1) give an overview of three-dimensional vortex evolution; strong PV gradients demark the vortex edge. In early September, strong MLS trace-gas gradients at each isentropic level are apparent across the vortex boundary, as seen in N_2O and O_3 below ~ 1400 K, and in HCl below ~ 900 K. Chlorine was still activated on 3 September, but had converted to HCl by 15 October, at which time O_3 depletion had ceased [*Santee et al.*, 2005]. The 2004 vortex breakup progressed from the top down, as modeling and meteorological data studies [e.g., *Manney et al.*, 1994] indicate is typical in the SH, and as suggested in H_2O observations for 2002 [*Orsolini et al.*, 2005]. Low-latitude, high- N_2O , low-HCl air was transported into the polar regions at increasingly lower altitudes; O_3 shows high values in the midstratospheric peak intruding progressively further poleward. The vortex weakened in the upper stratosphere in late September, so that by 15 October strong PV and trace gas gradients were apparent only below ~ 900 K. By 22 November, a significant transport barrier existed only below ~ 600 K, with N_2O and HCl showing mid-EqL values transported to the pole near or below 700 K. Low N_2O values inside and along the vortex edge progressed downward through late November, indicating continuing descent. However, higher N_2O (lower HCl) in the vortex core on 22 November suggests ascent in this region (while mixing could increase (decrease) N_2O (HCl), such a change would be expected to extend to, and even be strongest at, the vortex edge). The beginning of ascent is evident in N_2O below ~ 600 K on 15 October at highest EqLs, consistent with GEOS-4 diabatic descent rates, which show weak ascent starting in the lower stratospheric vortex core by early October, and with model calculations [e.g., *Manney et al.*, 1994].

Figure 2 shows timeseries at 850 K in the middle stratosphere of effective diffusivity (K_{eff}) calculated from GEOS-4 PV and MLS N_2O , H_2O and O_3 . K_{eff} , expressed as log-normalized equivalent length, measures the complexity of tracer contours; high values indicate mixing regions and low values transport barriers [e.g., *Allen and Nakamura*, 2001]. Very low K_{eff} coincident with strong PV gradients shows the polar vortex transport barrier. Episodic increases in mid-EqL

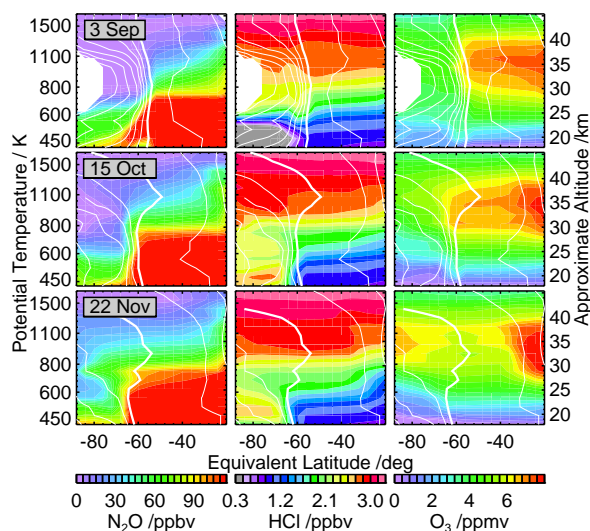


Figure 1. Equivalent Latitude (EqL)/potential temperature cross-sections of MLS N_2O , HCl, and O_3 during the 2004 SH vortex breakup. Overlaid contours are scaled potential vorticity (sPV, *Manney et al.* [1994]).

(extravortex) mixing in early and mid-September are associated with minor warmings, common in the SH late winter [e.g., *Lahoz et al.*, 1996], that have little effect on vortex strength. At the end of September, a large increase in mid-EqL mixing accompanied by a weakening vortex transport barrier (increasing K_{eff} , diverging PV contours) signals vortex erosion leading to the breakup. The vortex edge remains distinct until mid-October, when the isolated area rapidly retreats to the pole, accompanied by large mixing over a broad EqL range. By early November, the vortex has broken up and the transport barrier is no longer apparent (PV gradients are weak and K_{eff} is high throughout the hemisphere).

The timeseries of MLS N_2O (H_2O) shows episodic decreases (increases) in mid-EqL values during periods of stronger mixing, and erosion of low (high) values characteristic of the vortex as the transport barrier dissipates. Also apparent in early September and early October is higher N_2O extending from low into mid-EqLs, signaling poleward transport when increasing K_{eff} indicates enhanced mid-EqL mixing. Similar features are seen in O_3 (notably in early October), with the poleward transport of low latitude air quite distinct since O_3 has very strong subtropical gradients. MLS trace gas transport thus corresponds closely to expectations from GEOS-4 analyses and calculated mixing. Mid-EqL O_3 decreases after poleward transport via formation of “low-ozone pockets” (see below). The return of low O_3 values at high EqL after the vortex breakup shows the onset of summer photochemistry [e.g., *Luo et al.*, 1997].

850-K maps (Figure 3) show the detailed evolution as-

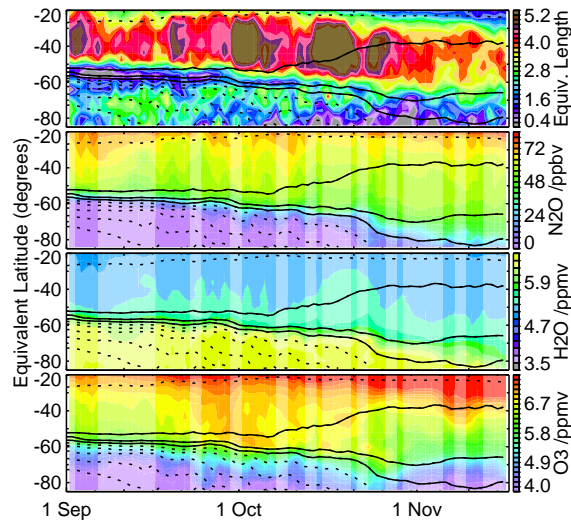


Figure 2. EqL-time series of K_{eff} (expressed as equivalent length, see text) and MLS N_2O , H_2O and O_3 at 850 K (~ 30 km) during the SH 2004 vortex breakup. Paler colors show where the estimated precision from the Kalman filter smoothing is poor because some days of MLS data were not processed [Santee et al., 2005]. Overlaid contours are sPV, with solid contours in vortex edge region.

sociated with vortex decay (N_2O morphology, not shown, is very similar to that of H_2O). Before the vortex begins to decay (e.g., 1 October), air is drawn up from low latitudes, around the vortex and into an anticyclone, and filaments are drawn off the vortex. These extrusions from different air masses are apparent in MLS trace gases and correspond closely to features in GEOS-4 PV. When low-latitude ozone is drawn into and confined in the anticyclone, it relaxes photochemically to values characteristic of high latitudes (e.g., 23 October), forming a low-ozone pocket [e.g., Manney et al., 1995], a common winter/spring phenomenon [e.g., Harvey et al., 2004]. This relaxation of mid-latitude O_3 values, along with stronger subtropical O_3 gradients, makes some tropical tongues more apparent in O_3 than in H_2O (e.g., 23 October). The vortex continues to erode, with tongues of low-latitude and vortex air mixing in midlatitudes, until only weak fragments with vortex-like trace gas values remain in late November. Higher ambient midlatitude H_2O values in late November signify mixing of air originally from the vortex. Consistent with model studies [e.g., Hess, 1991; Orsolini, 2001], small vortex fragments persist through December (not shown), long after the main vortex breakup, in both MLS data and GEOS-4 PV.

K_{eff} and MLS trace gas timeseries show a much later breakup of the lower stratospheric vortex (Figure 4). Enhanced mixing beginning in mid-September is limited to mid-EqLs, with little weakening of the vortex until after mid-November. By early December, the vortex weakens sig-

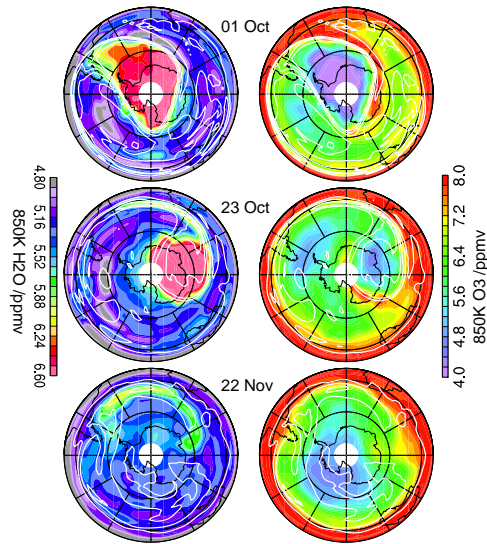


Figure 3. Maps of 850 K MLS H_2O and O_3 during the vortex breakup. Overlaid contours are sPV. Domain is 0 to 90°S with 0° longitude at the top and 90°E to the right; fine lines show 30 and 60°S latitudes.

nificantly, then quickly shrinks and disappears. Beginning in early October, lower N_2O (higher HCl) values characteristic of the vortex edge extend to lower EqLs, consistent with increases in mixing seen in K_{eff} . After chlorine deactivation in early October [Santee et al., 2005], HCl provides an excellent tracer of vortex evolution in the lower stratosphere, with very sharp gradients across the vortex edge. The onset of increased mid-EqL mixing in October, vortex erosion, and dispersal of vortex air in November are illustrated clearly in HCl and N_2O . The same processes are apparent in O_3 , with high collar values along the vortex edge first mixing out into lower EqLs in October and early November and later being diluted as O_3 -depleted air is exported from the decaying vortex.

Figure 5 details the lower stratospheric vortex breakup, with MLS daily global HCl observations affording an exceptional view of the dispersal of vortex air. During October, the vortex is strong, but distorted and mobile, with filaments drawn off and mixed into midlatitudes (e.g., 15 October); such events result in increasing extravortex HCl (e.g., 23 November). Filamentation in MLS observations is consistent with that in GEOS-4 PV fields. By 23 November the vortex has weakened and shrunk, and an intrusion of air from near the edge deep into the vortex is apparent; such events are less common than air drawn off the vortex, but play a role in mixing and vortex erosion during the spring breakup. Between 5 and 11 December, the vortex breaks into three major fragments that subsequently decay and drift into lower latitudes, some quickly moving to the subtropics, as has been

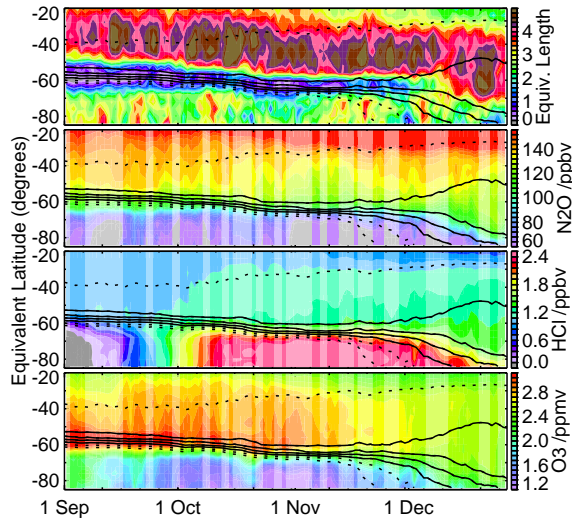


Figure 4. As in Figure 2, but at 520 K, and showing MLS N₂O, HCl, and O₃.

noted in model studies of northern hemisphere (NH) vortex breakup [Piani et al., 2002]. A vortex remnant still exists on 28 December, but none can be identified a few days later, reminiscent of the short persistence of lower stratospheric vortex remnants in model studies of late NH final warmings [Vaugh and Rong, 2002]. Poorer correspondence between small vortex fragments and PV contours may indicate resolution issues or may suggest less accuracy in these detailed features in the GEOS-4 PV; future analyses of these features will improve understanding of dispersal of vortex remnants and representation of these processes in models.

Figure 6 shows the subvortex (the lower reaches of the vortex where it is more permeable, below ~400 K [McIntyre, 1995]) at 370 K, just below the tropical tropopause. The subvortex abruptly dissipates in mid-late December, only a few days later than the vortex at 520 K (Figure 4). MLS data in January (not shown, as they were processed with different software) confirm the continuing consistency of trace gas evolution with that of K_{eff} and PV. 370 K H₂O maps (Figure 7) show slightly larger, more coherent fragments directly underlying those at 520 K (Figure 5), with good correspondence between MLS data and GEOS-4 PV. In a NH modeling study, Piani et al. [2002] found that air from the decaying subvortex remained confined to higher latitudes than it did at higher altitudes, analogous to the evolution seen in SH MLS data.

3. Summary

MLS on Aura allowed an unprecedentedly detailed view of transport during the 2004 vortex breakup by providing

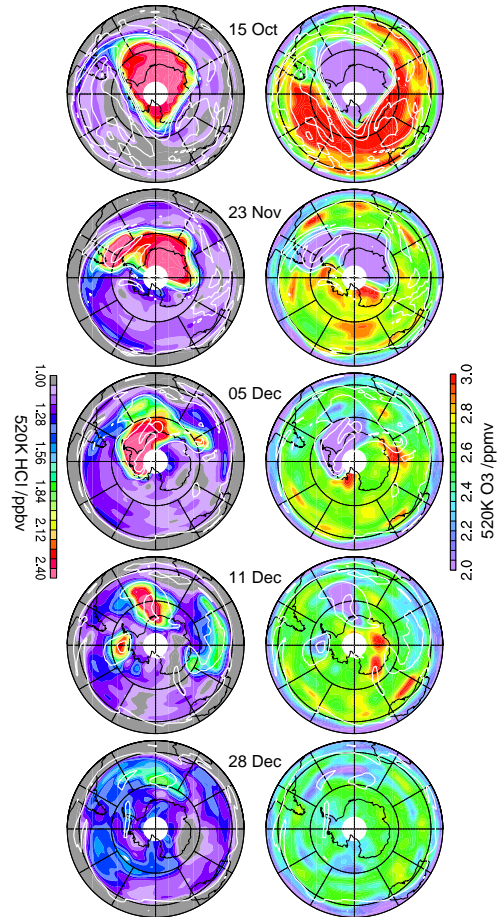


Figure 5. Maps of 520 K MLS HCl and O₃ showing the lower stratospheric vortex breakup. Layout is as in Figure 3.

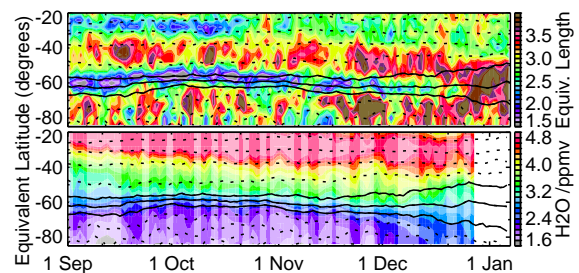


Figure 6. As in Figure 2, but at 370 K (~12 km), and showing MLS H₂O. MLS data after 28 December were processed with new software and are not shown.

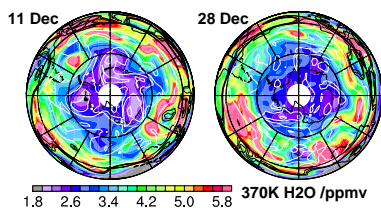


Figure 7. Maps of 370 K MLS H₂O; layout is as in Figure 3. Tropospheric air is equatorward of black PV contours.

daily global measurements of several tracers over the full stratosphere and time period of the final warming. The MLS data show low-latitude air moving into high latitudes at progressively lower levels as the vortex broke up, disappearing in the upper stratosphere by early October, in the midstratosphere by the end of October, and in the lower stratosphere by late December. The subvortex broke up immediately after the lower stratospheric vortex. MLS N₂O and HCl observations show diabatic descent continuing through November in most of the vortex, but weak ascent beginning in the lower stratospheric vortex center after mid-October. HCl is a particularly valuable tracer of vortex evolution during spring in the SH lower stratosphere, showing clearly filamentation and mixing during the breakup, rapid disappearance of vortex fragments afterward, and close correspondence between MLS data and GEOS-4 PV. In contrast to the lower stratosphere, MLS N₂O and H₂O show vortex fragments in the middle stratosphere persisting over a month after the breakup. MLS trace gas evolution shows good consistency with mixing calculated from GEOS-4 data and with modeling studies. By providing information on the whole stratosphere and complete breakup period, for several key trace gases, the EOS MLS data have enabled a unique examination of transport during the vortex breakup in Austral spring 2004, a view that has previously been possible only in model studies. Future studies using MLS data offer additional advances in understanding the detailed processes involved in the polar vortex breakup in both hemispheres.

Acknowledgments. Thanks to NASA's Global Modeling and Assimilation Office for GEOS-4 data. Work at the Jet Propulsion Laboratory, California Institute of Technology, was done under contract with the National Aeronautics and Space Administration.

References

- Ajtić, J., et al. (2004), Dilution of the Antarctic ozone hole into southern midlatitudes, 1998–2000, *J. Geophys. Res.*, *109*, doi:10.1029/2003JD004500.
- Allen, D. R., and N. Nakamura (2001), A seasonal climatology of effective diffusivity in the stratosphere, *J. Geophys. Res.*, *106*, 7917–7935.
- Bloom, S. C., et al. (2005), The Goddard Earth Observing Data Assimilation System, GEOS DAS Version 4.0.3: Documentation and validation, *Tech. Rep. 104606 V26*, NASA.
- Harvey, V. L., et al. (2004), On the distribution of ozone in stratospheric anticyclones, *J. Geophys. Res.*, *109*, D24,308, doi:10.1029/2004JD004992.
- Hess, P. G. (1991), Mixing processes following the final stratospheric warming, *J. Atmos. Sci.*, *48*, 1625–1641.
- Lahoz, W. A., et al. (1996), Vortex dynamics and the evolution of water vapour in the stratosphere of the southern hemisphere, *Q. J. R. Meteorol. Soc.*, *122*, 423–450.
- Luo, M., et al. (1997), An analysis of HALOE observations in summer high latitudes using air mass trajectory and photochemical model calculations, *J. Geophys. Res.*, *102*, 16,145–16,156.
- Manney, G. L., et al. (1994), On the motion of air through the stratospheric polar vortex, *J. Atmos. Sci.*, *51*, 2973–2994.
- Manney, G. L., et al. (1995), Formation of low-ozone pockets in the middle stratospheric anticyclone during winter, *J. Geophys. Res.*, *100*, 13,939–13,950.
- McIntyre, M. E. (1995), The stratospheric polar vortex and subvortex: Fluid dynamics and midlatitude ozone loss, *Phil. Trans. R. Soc. Lond. A*, *352*, 277–240.
- Orsolini, Y. J. (2001), Long-lived tracer patterns in the summer polar stratosphere, *Geophys. Res. Lett.*, *28*, 3855–3858.
- Orsolini, Y. J., et al. (2005), An observational study of the final breakdown of the southern hemisphere stratospheric vortex in 2002, *J. Atmos. Sci.*, *62*, 735–747.
- Piani, C., et al. (2002), Transport of ozone-depleted air on the breakup of the stratospheric polar vortex in spring/summer 2000, *J. Geophys. Res.*, *107*, 8270 doi:10.1029/2001JD000488.
- Santee, M. L., et al. (2005), Polar processing and development of the 2004 Antarctic ozone hole: First results from MLS on Aura, *Geophys. Res. Lett.*, *32*, doi:10.1029/2005GL022582, in press.
- Waters, J. W., et al. (1999), The UARS and EOS Microwave Limb Sounder (MLS) experiments, *J. Atmos. Sci.*, *56*, 194–218.
- Waugh, D. W., and P. Rong (2002), Interannual variability in the decay of lower stratospheric Arctic vortices, *J. Meteor. Soc. Japan*, *80*, 997–1012.
- G. L. Manney (corresponding author), Department of Natural Sciences, New Mexico Highlands University, Las Vegas, NM 87701. (e-mail: manney@mls.jpl.nasa.gov
- M. L. Santee, L. Froidevaux, N. J. Livesey, W. G. Read, and J. W. Waters, Jet Propulsion Laboratory, Mail Stop 183–701, 4800 Oak Grove Drive, Pasadena, CA 91109.
- H. C. Pumphrey, University of Edinburgh, UK.
- S. Pawson, NASA/Goddard Space Flight Center, Code 610.1, Greenbelt, MD 20771.